

RESEARCH PAPER

THEORETICAL AND EXPERIMENTAL MODELING OF THE PROCESS OF MELTING COMPLEX ALLOYED STEELS (Fe-Si-Al-Mn)

Bauyrzhan Kelamanov ^{1,*}, Yerbol Kyatbay ², Gaukhar Yerekeyeva ², Tair Tushyev ²

¹ Aktobe Regional University Named After K. Zhubanov, Department of Metallurgy and Mining, A. Moldagulova Street No. 34, 030000, Aktobe, Kazakhstan

² Karaganda Industrial University, Department of Metallurgy and Materials Science, Republic Street No 30. 101400, Temirtau, Kazakhstan

*Corresponding author: kelamanovb84@gmail.com, tel: + 77014965196, Department of Metallurgy and Mining, Aktobe Industrial University Named After K. Zhubanov, A. Moldagulova Street No. 34, 030000, Aktobe, Kazakhstan.

Received: 30.03.2024

Accepted: 12.05.2024

ABSTRACT

The thermodynamic-diagram analysis method has proven to be a valuable tool in the realm of complex theoretical research of multi-component systems. This method simplifies the study of phase transformations in multicomponent systems by breaking them down into thermodynamically stable elementary partial subsystems of equal dimensionality as the main ones. The practical implications of this approach, as evidenced by studies in the field of refractories and ferroalloys production, are significant. It aids in interpreting chemical interactions in complex systems, thereby contributing to the development and optimisation of manufacturing processes. Technological research was carried out in an ore-thermal furnace with a capacity of 150 kVA. As a result of the study, quantitative data were obtained on the ratio of components of complex alloys with an average content, %: Mn – 26-50; Si – 30-48; Al – 2-3; Fe – 15-21.

Keywords: Melting Complex Alloyed Steels, thermodynamic diagram, Gibbs energy, phases, mathematical model.

INTRODUCTION

Our research delves into the intricate phase relationships in multi-component systems, a pivotal area of advancing and optimising metallic material manufacturing processes. In this vein, the innovative use of thermodynamic diagram analysis emerges as a critical player, offering insights into phase compositions and structures under diverse conditions. This paper unveils a unique study of the Fe-Si-Al-Mn system, employing thermodynamic-diagram analysis to construct phase relationship diagrams for distinct components of this system [1-5].

A phase diagram is essential for visualising different phases, their distribution, and composition at various temperatures and compositions. In this study, phase diagrams were constructed for individual parts of the Fe-Si-Al-Mn system. This allows for a more comprehensive understanding of phase transformations and relationships between components (Table 1).

Table 1 Initial Thermodynamic Data in the Fe-Si-Al-Mn System

| Phases | ΔH_{298}^0 / kJ/mol | S_{298}^0 kJ/mol | ΔG_{298}^0 kJ/mol |
|---------------------------------|-----------------------------|--------------------|---------------------------|
| FeAl ₂ | - 78,24 | 83,37 | - 103,08 |
| FeSi | - 76,57 | 46,02 | - 76,58 |
| FeSi ₂ | - 76,15 | 55,23 | - 73,29 |
| Fe ₂ Si ₃ | - 81,97 | 78,14 | - 105,25 |
| MnAl ₄ | - 106,69 | 146,35 | - 150,30 |
| MnAl ₆ | - 87,86 | 194,58 | - 145,85 |
| Mn ₃ Si ₃ | - 273,22 | 235,56 | - 278,89 |
| MnSi | - 77,82 | 47,07 | - 76,70 |

In general, the study of thermodynamic-diagram analysis of the Fe-Si-Al-Mn system, including the construction of phase diagrams and the development of mathematical models for complex alloys, represents a significant contribution to the advancement of scientific and technological achievements in the fields of metallurgy and materials science. It opens up new possibilities for creating innovative materials with improved properties and enhanced performance, which contributes to the development of various industrial sectors and the progress of society.

This study employs the thermodynamic-diagram methods to construct phase composition diagrams in the Fe-Si-Al-Mn system. These methods are widely used in research and provide valuable information about phase relationships under various conditions [6].

This work uses a balanced method based on proprietary development to describe the phase composition diagram mathematically [7]. This method allows for considering interactions between components and constructing a mathematical model that operates in a multidimensional space, thereby accommodating a more significant number of components than the three-dimensional space typically used for diagram construction [8].

MATERIAL AND METHODS

An additive method was utilised to calculate standard Gibbs energy (Table 2). The paper provides an example of calculating the standard Gibbs energy for the ternary phase Mn₄Al₅Si₂, where MnAl₃, Mn₂Si, and MnSi are constituents. The calculation demonstrates that the standard Gibbs energy for this ternary phase is -321.455 [9].

Thus, this study uses computational methods to construct phase composition diagrams and determine the energetic parameters of ternary phases. These methods enable a more accurate description of phase relationships and calculations in multicomponent systems, such as the Fe-Si-Al-Mn system.

Table 2 Calculation of Standard Gibbs Energy Using the Additive Method

| Phase | $\Delta G^{\circ}298$ / kJ/mol |
|-------------------|--------------------------------|
| $Mn_4Al_3Si_2$ | - 321 455 |
| Mn_2Al_6Si | - 561 735 |
| Mn_3Al_6Si | - 375 075 |
| Fe_2Al_2Si | - 179,86 |
| $FeAl_2Si$ | - 99,79 |
| $FeAl_3Si$ | - 141,47 |
| $Fe_3Al_{11}Si_6$ | - 753,77 |
| $Fe_3Al_{14}Si_3$ | 886,17 |

When investigating the metallic system Fe-Si-Al-Mn using the thermodynamic diagram analysis (TDA) method [10-13], an important step is dividing boundary subsystems into elementary tetrahedra. This approach allows for a more precise analysis of phase relationships and system properties.

This study described compounds of varying complexity that are part of the Fe-Si-Al-Mn system. Describing these compounds allows for determining their structure and properties, which is essential for understanding the system's phase transformations. The study results are presented in Fig. 1, which shows tetrahedra of congruently and incongruently melting compounds in the Fe-Si-Al-Mn system. This visualisation of the diversity of structures and compounds indicates their stability in this system.

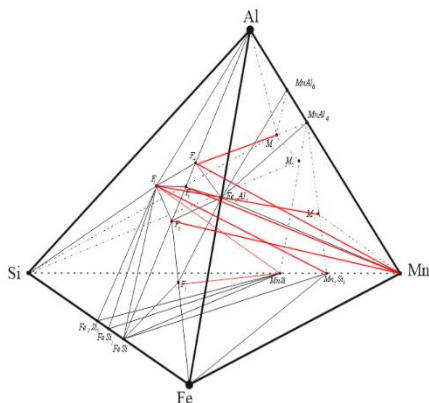


Fig. 1 Tetrahedra of the metallic system Fe-Si-Al-Mn
 $M_1 - Mn_4Al_3Si_2$, $M_2 - Mn_2Al_6Si$, $M_3 - Mn_3Al_6Si$

During the breakdown of the entire Fe-Si-Al-Mn system, congruent melting compounds were considered, and metastable nodes of incongruent components were grouped into stable tetrahedra. An important aspect was to ensure that the sum of the relative volumes of elementary tetrahedra was equal to one, confirming the correctness of the breakdowns conducted.

Based on the tetrahedra of four partial ternary systems, Fe-Si-Al, Fe-Mn-Al, Fe-Mn-Si, and Mn-Al-Si, a phase composition diagram of the four-component system Fe-Si-Al was constructed. A Si-Al-Mn system was also built, representing a ternary system [14-17].

Two methods of constructing the phase composition diagram were used to determine the elementary tetrahedra constituting

this system. The first method, geometric, proved very complex due to the many emerging phases and intersections of triangle boundaries. Instead, the process of closing triangles on a tetrahedron was applied.

This method involves finding triangles where two out of three phases coincide. If two triangles from the nearest ternary subsystem have two identical phases, they form a tetrahedron, and so on. This approach was used to find the phase compositions of the second and third columns. Eight tetrahedra were obtained using this method.

Thus, closing triangles on a tetrahedron allowed us to determine eight elementary tetrahedra constituting the Fe-Si-Al-Mn system. These results are essential in understanding this metallic system's phase relationships and structural features. Using this method, eight tetrahedra were obtained:

- Fe-FeSi-Fe₂Al₂Si-Mn
- Fe₃Al₁₁Si₆-Si-MnSi
- Fe₂Si₅-FeSi₂-Fe₃Al₁₁Si₆-MnSi
- FeSi-FeSi₂-Fe₃Al₁₁Si₆-MnSi
- Fe-Mn-FeSi-Fe₂Al₂Si
- MnAl₆-Fe₂Al₅-Al-Mn₂Al₆Si
- MnAl₄-MnAl₆-Fe₂Al₅-Mn₂Al₆Si
- Mn-MnAl₄-Fe₂Al₅-MnAl₅Si₂

When analysing the compositions of high-percentage complex alloy (Fe-Si-Al-Mn) obtained from high-silica manganese ore from the "Zapadny Kamys" deposit and high-ash coal from the Karaganda coal basin, using the calculated transformation equations, the following was established:

1) The composition of the aluminium-rich complex alloy (Fe-Si-Al-Mn), for which the transformation equations for calculating the equilibrium ratios of secondary components through the primary component are expressed as a system of four linear equations, is determined as follows:

$$FeAl_3 = 2,44942 \cdot Fe;$$

$$Al = -1,44942 \cdot Fe + 1,0 \cdot Al;$$

$$Si = 1,0 \cdot Si - 0,88303 \cdot Mn;$$

$$Mn_{11}Si_{19} = 1,88303 \cdot Mn.$$

From here, it follows that this complex alloy (Fe-Si-Al-Mn) in the sub-solidus state includes phases, %: FeAl₃=36,74; Al=3,26; Si=41,17; Mn₁₁Si₁₉=18,83.

2) compositions of low-aluminium percentage complex alloy (Fe-Si-Al-Mn) (Fe-20; Si-40; Al-10; Mn-30), as well as compositions of the complex alloy (Fe-Si-Al-Mn), obtained using coals from the Karaganda and Ekibastuz coal basins. The calculation of equilibrium ratios of secondary components for alloys located within it is carried out according to the transformation equations expressed as a system of four expressions:

$$Fe_2Al_5 = 1,82792 \cdot Al;$$

$$FeSi_2 = -1,66066 \cdot Al + 2,00582 \cdot Mn;$$

$$Si = -0,88303 \cdot Fe + 1,0 \cdot Si + 0,83274 \cdot Al - 1,00582 \cdot Mn;$$

$$Mn_{11}Si_{19} = 1,88303 \cdot Fe.$$

The alloy formed in the temperature range below the solidus will include phases, %: Fe₂Al₅=18,28; FeSi₂=43,57; Si=0,49; Mn₁₁Si₁₉=37,66.

It should be noted that the compositions of the previously melted complex alloy (Fe-Si-Al-Mn) with high (more than 30%) manganese content are in the tetrahedron region Fe₂Al₅-FeSi-FeSi₂-Mn₁₁Si₁₉ with a relatively small volume V=0.048469.

Thus, conducting thermodynamic diagram analysis (TDA) based on phase structure diagrams of multicomponent systems has allowed us to identify optimal alloy composition regions corresponding to the most favourable conditions for the melting process. These regions have a relatively large volume, as alloy composition modelling, such as tetrahedra, is more stable and technologically predictable.

Table 3 Initial Data on the Iron Crystallization Area in the Fe-Mn System

| T, K | X ^L _{Fe} | X ^S _{Fe} | X ^L _{Mn} | X ^S _{Mn} | a ^L _{Fe} /a ^S _{Fe} | a ^L _{Mn} /a ^S _{Mn} | Φ _{Fe} | Φ _{Mn} |
|------|------------------------------|------------------------------|------------------------------|------------------------------|--|--|-----------------|-----------------|
| 1746 | 0.875 | 0.904 | 0.125 | 0.096 | 0.96245 | 1.1321 | 1.1905 | 0.4757 |
| 1723 | 0.825 | 0.857 | 0.175 | 0.143 | 0.94884 | 1.1196 | 1.3798 | 0.5594 |
| 1698 | 0.766 | 0.799 | 0.234 | 0.201 | 0.93387 | 1.1058 | 1.6221 | 0.6616 |
| 1673 | 0.701 | 0.734 | 0.299 | 0.266 | 0.91869 | 1.0918 | 1.8435 | 0.7510 |
| 1648 | 0.633 | 0.665 | 0.367 | 0.335 | 0.90331 | 1.0775 | 2.0619 | 0.8186 |
| 1623 | 0.558 | 0.5876 | 0.442 | 0.4124 | 0.88773 | 1.0630 | 2.3040 | 0.8820 |
| 1598 | 0.48 | 0.5064 | 0.52 | 0.4936 | 0.87194 | 1.0483 | 2.5595 | 0.9053 |
| 1573 | 0.398 | 0.4206 | 0.602 | 0.5794 | 0.85594 | 1.0333 | 2.8165 | 0.8560 |
| 1548 | 0.315 | 0.333 | 0.685 | 0.667 | 0.83973 | 1.0180 | 3.1433 | 0.6712 |
| 1523 | 0.228 | 0.2416 | 0.772 | 0.7584 | 0.82331 | 1.0025 | 3.3556 | 0.1410 |
| 1518 | 0.209 | 0.2218 | 0.7906 | 0.7782 | 0.82000 | 0.9994 | 3.4494 | -0.0398 |

Processing the initial data according to **Table 3** allowed for the construction of a graph showing the dependence of the osmotic coefficient of Bjerrum-Guggenheim (**Fig. 2**) on the ratio of the activity of the liquid and solid phases of the ideal system.

To determine the physicochemical and metallurgical properties of the complex alloy, a series of research works were conducted: X-ray phase analysis of the alloy, determination of the density and melting temperature of the alloy using computational methods, which are essential criteria for assessing the production of complex alloys. The alloy's X-ray phase analysis was performed using a multifunctional Rigaku SmartLab X-ray diffractometer (manufactured in Japan). This multifunctional experimental setup allows for a wide range of tasks using various relevant X-ray techniques to investigate the structure of samples.

The primary purpose of the metallurgical evaluation and testing was to determine the possibility of obtaining a complex Fe-Si-Mn-Al alloy from the provided raw materials, develop technological modes, and obtain a non-scattering alloy from non-forming manganese-containing ores and high-ash coals.

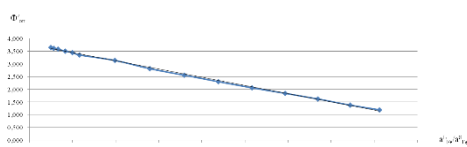


Fig. 2 Dependence of the osmotic coefficient of Bjerrum-Guggenheim Φ_{oi} for manganese on the activity ratio a^L_{Fe}/a^S_{Fe}

The data of this dependency were processed using the method of least squares by a specially developed program, resulting in the following mathematical expression for the osmotic coefficient of Bjerrum-Guggenheim Φ_{oi} for iron (30):

$$\Phi_{Fe}^i = 19,6707 - 19,6707 \cdot a_{Fe}^L / a_{Fe}^S \quad R_{xy} = -0,9992$$

Then, we perform a similar calculation for manganese, finding the equation describing the dependence Φ_{oi} of a^L_{Mn}/a^S_{Mn} according to **Fig. 3**.

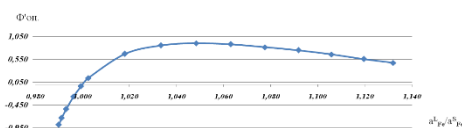


Fig.3 Dependence of the osmotic coefficient of Bjerrum-Guggenheim Φ_{oi} for manganese on the activity ratio a^L_{Mn}/a^S_{Mn}

RESULTS AND DISCUSSION

The charge calculation was conducted for 100 kg of coal. Solid carbon was ultimately calculated to reduce manganese ore oxides, and all ash oxides in the coal and excess carbon were neutralised by adding quartzite. Iron shavings were used in the composition of the charge materials to improve the process and as a one-time addition to disrupting carbide buildup in case of an excess reducing agent in the charge. Manganese-containing ores from the «Bogach» and «Esymzhal» deposits were used as manganese-containing ores. High-ash coals from the «Saryadyr» and «Zhamantuz» mines were used as reducing agents [18]. **Tables 4 and 5** present the chemical and technical analysis results of the initial charge materials for smelting.

Table 4 Technical Composition of Charge Materials

| Material | A ^c | V ^t | W ^t | C _{ra} |
|---------------------------|----------------|----------------|----------------|-----------------|
| High-ash coal «Saryadyr» | 50.04 | 19.28 | 1.98 | 31.86 |
| High-ash coal «Zhamantuz» | 52.405 | 3.940 | 1.250 | 42.405 |

Preparing the charge materials involved crushing them at a crushing and sorting site to a size of +5 -40 mm for the manganese ore from the «Bogach» and «Esymzhal» deposits and quartzite. The high-ash coals from the «Saryadyr», «Borly», and «Zhamantuz» mines were crushed to a fraction of +10 -40 mm. The length of the steel shavings was not more than 20 mm.

For conducting laboratory experiments on smelting a Fe-Si-Mn-Al alloy using manganese ores from the «Esymzhal» and «Bogach» deposits, high-ash coals from the «Zhamantuz» and «Saryadyr» mines, and coke, an ore-thermal laboratory furnace with a capacity of up to 150 kVA was constructed. The stove was designed based on an existing experimental ore-thermal furnace with a capacity of 250 kVA. Only the power transformer OSZ-250/0.5 UHL4 from the Moscow Transformer Plant was borrowed for operation. Cooling was provided by natural air. No-load tap changer (PBV). Frequency - 50 Hz. Insulation heat resistance class - F. Phases - 1. Winding connection scheme and group - 1/1-0. The transformer has seven voltage steps on the secondary side from 27.4 V to 71.2 V (**Table 6**).

In the new laboratory ore-thermal furnace, the following voltage steps on the secondary side were used according to the geometry of the bath and the diameter of the furnace electrodes: from 27.5V to 43.1V. The furnace bath's main characteristics are a diameter of 300 mm and a depth of 300 mm, and the graphite electrodes used have a diameter of 100 mm. The furnace bath is lined with fireclay bricks. The bottom of the furnace is filled with electrode mass and preheated to 100-120°C. The bath's surface has a slope at an angle of 5-7° towards the tapping hole to facilitate the discharge of the melt.

Table 5 Chemical composition of charge materials

| Material | Fe ₂ O ₃ | SiO ₂ | Al ₂ O ₃ | MnO ₂ | CaO | MgO | TiO ₂ | P ₂ O ₅ | S | LOI |
|---------------------------|--------------------------------|------------------|--------------------------------|------------------|-------|------|------------------|-------------------------------|-------|-------|
| High-ash coal «Saryadyr» | 5.79 | 66.36 | 20.7 | | 2.64 | 3.46 | 1.01 | 0.035 | 0.005 | |
| High-ash coal «Zhamantuz» | 1.02 | 67.05 | 17.5 | | 5.01 | 8.49 | 0.79 | 0.09 | 0.05 | |
| Material | Fe ₂ O ₃ | SiO ₂ | Al ₂ O ₃ | MnO ₂ | CaO | MgO | TiO ₂ | P ₂ O ₅ | S | LOI |
| Manganese ore «Bogach» | 5.72 | 6.27 | 0.72 | 49.94 | 15.05 | 0.83 | | 0.02 | 0.01 | 21.44 |
| Manganese ore «Esymzhal» | 3.29 | 9.27 | 0.82 | 46.48 | 17.2 | 0.71 | | 0.01 | 0.01 | 22.21 |
| Quartzite | 0.52 | 95.57 | | | 0.24 | 0.12 | | | 0.01 | 3.54 |

Table 6 Characteristics of the Ore-Thermal Furnace Transformer with a Capacity of 150 kVA

| Characteristic | Value |
|-------------------------------------|--------------------------|
| Manufacturer | Moscow Transformer Plant |
| Type | OSZ-250/0.5 UHL4 |
| Rated power | 150 kVA |
| Cooling | Natural air |
| No-load tap changer (PBV) | Yes |
| Frequency | 50 Hz |
| Insulation heat resistance class | F |
| Phases | 1 |
| Winding connection scheme and group | 1/1-0 |
| Voltage steps on the secondary side | 27.4 V to 71.2 V |

The main advantage of the constructed laboratory ore-thermal electric furnace is its lower energy and material consumption compared to semi-industrial furnaces with a power of 150 kW while solving the same technological tasks. Tests were conducted to address the following objectives:

- Testing the smelting technology of complex alloy based on Fe-Si-Mn-Al in the laboratory ore-thermal furnace.
- Checking and testing the melting unit's loading mode and the ore-thermal furnace's electrical circuit with a power of up to 150 kW. Laboratory tests for smelting complex alloys were conditionally divided into the following periods:
- Preheating the electric furnace and bringing it into operation.
- Smelting of complex alloy based on Fe-Si-Mn-Al using high-ash coal from the "Zhamantuz" mine and manganese ore from the "Esimzhal" deposit.
- Smelting of complex alloy based on Fe-Si-Mn-Al using high-ash coal from the "Saryadyr" mine and manganese ore from the "Bogach" deposit.

Smelting of complex alloy based on Fe-Si-Mn-Al using high-ash coal from the "Saryadyr" mine. Overall, the furnace operation was characterised by stable performance and active metal output in all three smelting periods. The extraction of critical elements was as follows (in mass %): Si – 75-85, Al – 60-70, and Mn – 80-87. Each batch of metal was weighed, and samples were taken according to GOST 17260-87 for chemical composition analysis. Chemical analysis of the samples was performed according to GOST 22772.4-77, GOST 22772.6-77, and GOST

22772.7-96. The average weighted chemical composition of the complex alloy is presented in **Table 7**.

Table 7 Chemical composition of complex alloyed steels (Fe-Si-Al-Mn), %

| Variant | Chemical composition, % | | | |
|---------|-------------------------|-------|-------|------|
| | Fe | Si | Mn | Al |
| I | 12,95 | 30,23 | 50,42 | 3,73 |
| II | 18,03 | 48,87 | 26,57 | 3,54 |
| III | 16,25 | 37,98 | 40,48 | 2,78 |

The smelting of complex ligature using high-ash coal from the Zhamantuz mine and manganese ore from the Yesymzhal deposit, high-ash coal from the Saryadyr mine and manganese ore from the Bogach deposit, and high-ash coal from the Saryadyr mine, as a whole, provided satisfactorily the output to the working technological mode.

Thus, the experimental tests indicate the possibility of smelting complex alloys based on Fe-Si-Mn-Al using the charge-containing materials mentioned above.

The results of experimental tests on a newly developed ore-thermal furnace with a capacity of up to 150 kVA established a stoichiometric coefficient (Ksto.) and a carbon excess coefficient (Ksto) using manganese ores Ksto —1.0.

The charge on the bath grate was not sintered, and its processing was carried out without difficulty. By the end of the period, opening the letterhead was much easier. The melt yield of the complex ligature was active.

The melting unit, the electrical circuit from the transformer to the electrode, withstands the load during the smelting of complex alloys and operates in a stable mode, as shown by the sensors of the ammeter and voltmeter devices [19-21].

It is recommended that comparative large-scale laboratory tests be carried out on a furnace with a capacity of 150 kVA using high-ash coals from the Saryadyr mine and manganese ore «Bogach» to refine the technology of smelting complex alloys based on Fe-Si-Mn-Al and improve technological indicators.

Radiographs of the obtained complex alloyed alloys (Fe-Si-Al-Mn) are shown in **Fig. 4**.

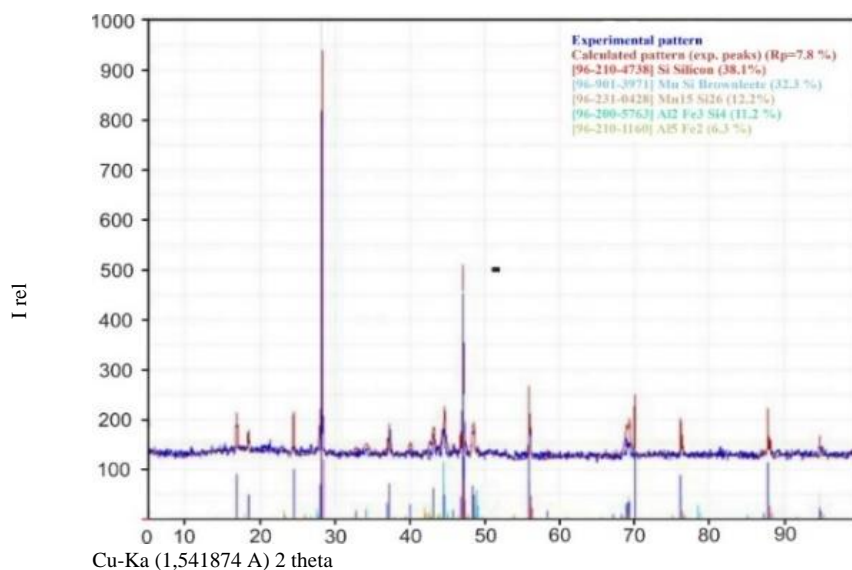


Fig. 4 X-ray of complex alloyed alloys (Fe-Si-Al-Mn)

The results of X-ray phase analysis of complex ligature prototypes confirm the presence of the following phases and compounds: $Mn_{15}Si_{26}$, $MnSi$, $Fe_3Al_2Si_4$, Fe_2Al_5 and free silicon Si.

CONCLUSION

The smelting of complex alloyed Fe-Si-Mn-Al alloys in a new furnace with a capacity of 150 kVA showed positive characteristics in high-temperature conditions. The sensors of the ammeter and voltmeter devices work in a stable mode. Melting was carried out at a voltage of 27.4 V, with a current load of 1000-1500 A. The extraction of the leading elements was (in % by weight): Si – 75-85, Al – 60-70 and Mn – 80-87. Experimental tests indicate the fundamental possibility of smelting complex alloys using the presented charge materials based on Fe-Si-Mn-Al. The melting unit, the electrical circuit from the transformer to the electrode, withstands the load during the smelting of complex alloys.

The main characteristics of a prototype of complex alloyed alloys (Fe-Si-Mn-Al) have been studied by methods of physico-chemical analysis. According to the results of the X-ray diffractometer of the prototypes, the phase composition was revealed: $Mn_{15}Si_{26}$, $MnSi$, $Fe_3Al_2Si_4$, Fe_2Al_5 and free silicon Si. The obtained prototypes of complex alloyed alloys (Fe-Si-Mn-Al) did not crumble during long-term storage, because in the phase composition of complex alloyed alloys (Fe-Si-Mn-Al) no $FeSi_2$ (leboite) compounds were found. The density of new types of calcium-containing ferroalloys is $3.96\div 4.52\text{ g/cm}^3$. The melting point is 1540-1560 K.

Acknowledgements: This work was carried out as part of a study funded by the Science Committee of the Ministry of Science and Higher Education of the Republic of Kazakhstan (grant no. AP 13068023)

REFERENCES

1. S. Baisanov, V. Tolokonnikova, G. Narikbayeva, I. Korsukova, Ye. Mukhambetgaliyev: *Metalurgija*, 59(3), 2020, 343-346.
2. V.V. Tolokonnikova, S.O. Baisanov, G. Yerekeyeva, G.I. Narikbayeva, G.S: *CIS Iron & Steel Review*, 24(1), 2022, 79-83. <https://doi.org/10.17580/cisir.2022.02.12>.
3. Y. Makhambetov, A. Abdirashit, Y. Kuvatbay, A. Yerzhanov: *Metalurgija*, 61(3-4), 2020, 804-806.
4. Y. Makhambetov, A. Abdirashit, Y. Kuvatbay, A. Yerzhanov: *Metalurgija*, 61(3-4), 2020, 807-809.
5. B. Kelamanov, Y.E. Samuratov, A. Akuov, et al.: *Metalurgija*, 61(1), 2022, 261-264.
6. B. Kelamanov, Y.E. Samuratov, Y. Zhumagaliyev, et al: *Metalurgija*, 59(1), 2020, 101-104.
7. A. I. Kazakov, V. I. Mokritskiy, V. I. Romanenko, L. Khitova. *Calculation of phase equilibria in multi-component systems*. Moscow: *Metalurgiya*, 1987, p. 136.
8. N.V. Ageev: *Calculations and experimental methods of building the state diagrams*. Moscow: *Nauka*. 1985.
9. M.A. Zakharov: *Vestnik Novgorodskogo gosudarstvennogo universiteta*, (98)7, 2016, 22-26.
10. K.Yu. Shakhnazarov: *Vestnik Magnitogorskogo gosudarstvennogo tekhnicheskogo universiteta im. G. I. Nosova*, 14(3), 2016,71-77.
11. V.P. Malyshev, A.M. Makasheva: *Russian Chemical Bulletin*, 69, 2020, 1296-1305. <https://doi.org/10.1007/s11172-020-2901-9>.
12. A.M. Makasheva, V.P. Malyshev: *Russian Metallurgy (Metally)*, 2021, 2021, 176-180. <https://doi.org/10.1134/S0036029521020154>.
13. T.M. Hansen, K.S. Cordua, K. Mosegaard: *Computational Geosciences*, 16, 2012, 593-611. <https://doi.org/10.1007/s10596-011-9271-1>.
14. I.K. Nikolaidis, A. Poursaeidesfahani, Z. Csaszar, et al.: *AIChE Journal*, 65(2), 2019, 792-803.

15. H. Gomez, M. Bures, A. Moure: Philosophical Transactions A, 377, 2019, 20180203. <https://doi.org/10.1098/rsta.2018.0203>.
16. S.O. Baisanov, V.V. Tolokonnikova, G.I. Narikbaeva: Title of the presentation. In.: *XX Mendeleev meeting on general and applied chemistry*. Nauka: Ekaterinburg, 2016. p. 137-138.
17. A.E. Vol: *Structure and properties of binary metallic systems, in 4 volumes*. Fizmatgiz: Moscow, 1962.
18. T. Zhuniskaliyev, A. Nurumgaliyev, O. Zayakin, et al.: Metallurgija, 59(4), 2020, 521-524.
19. E.K. Mukhambetgaliev, A.B. Esenzhulov, V.E. Roshchin: Steel in Translation, 48(9), 2018, 547-552. <https://doi.org/10.3103/S0967091218090097>.
20. A. Nurumgaliyev, T. Zhuniskaliyev, V. Shevko, et al.: Scientific Reports, 14, 2024, 7456. <https://doi.org/10.1038/s41598-024-57529-6>.
21. A. Nurumgaliyev, O. Zayakin, T. Zhuniskaliyev, B. Kelamanov, Y. Mukhambetgaliev: Metallurgist, 67(7-8), 2023, 1178-1186. <https://doi.org/10.1007/s11015-023-01609-x>.